Working Paper

The Speed–Density Relationship:
Road Traffic Flow Analysis with Spatial Panel Data

Koji KARATO, Naohito SATO and Tatsuo HATTA

Working Paper No. 246
November 30, 2009

FACULTY OF ECONOMICS
UNIVERSITY OF TOYAMA

3190 Gofuku, Toyama
930-8555 JAPAN

The Speed–Density Relationship: Road Traffic Flow Analysis with Spatial Panel Data[†]

Koji KARATO[‡]
Faculty of Economics, University of Toyama
Naohito SATO
Graduate School of Public Policy, University of Tokyo
Tatsuo HATTA
National Graduate Institute for Policy Studies

November 30, 2009

Abstract

In this paper, we focus on the fundamental speed–density relationship of aggregated vehicular traffic flow in the entire urban area. We use aggregated observations on routes that are treated as cross-section units in three time intervals and examine the speed–density relationship. We consider a variety of routes and road networks for our spatial panel data analysis. We apply the estimator of Kelejian and Prucha (1999) to the usual panel data case, based on certain restrictions on the evolution of spatial dependence over time.

JEL Classification: C31, C33, R41
Keywords: traffic flow theory, speed–density relationship, spatial panel data, generalized moments estimator

[†] This study was partly supported by KAKENHI: a Grant-in-Aid for Young Scientists (B) (#21730190) of the Japanese Ministry of Education, Culture, Sports, Science and Technology.
[‡] Corresponding author: 3190 Gofuku Toyama 930-8885 JAPAN, e-mail: kkarato@eco.u-toyama.ac.jp

1. Introduction

As traffic density increases, a road gets congested, and the speed of the traffic decreases. Since Greenshield's (1935) seminal paper, various models have been proposed to analyze the speed–density relationship. Much effort has been devoted to improving the oversimplified relationship specified by Greenshield. These classical studies, including those of Greenberg (1959), Underwood (1961), Gazis et al. (1961) and Drake *et al*. (1967), are limited to particular expressways and sections thereof. Moreover, the time period covered is also limited. Thus, this approach is arguably inadequate for understanding the speed–density relationship of toll-free roads in an entire urban area.

In this paper, we focus on the speed–density relationship of toll-free roads of the entire city. We estimate this relationship using the time-series cross-section data of several toll-free roads in the twenty-three ward district of Tokyo. Each road section, which is a cross-section observation unit, has a spatial linkage to other sections. Hence this data is likely to have spatial autocorrelation of the disturbances across cross-sectional units. Kelejian and Prucha (1999) developed an estimation method in terms of generalized moments applicable in the presence of spatial autocorrelation.

We extend their method for a time series cross section model so that the extended method can be applied to our data. The use of a time series data can effectively reduce the estimation bias cased by omitted variables that could take place when single time data is used.

The rest of the paper is organized as follows. In Section 2, we describe the classical speed–density relationship and outline traffic flow theory. In Section 3, we describe the empirical model used to estimate the speed–density relationship with spatial panel data. In Section 4, we explain key features of the data. In Section 5, we report our estimation and testing

results. Conclusions and potential directions for future work are discussed in Section 6.

2. The Speed–Density Relationship Model

Since Greenshield's (1935) seminal paper, the various models of the speed–density relationship have developed into the so-called *K*–*V* curve in a traffic stream model, according to which speed *V* decreases as traffic density *K* increases. Researchers have long been interested in functionally specifying and estimating these relations. In our paper, the traffic density on a particular section of road is defined as hourly aggregated traffic flow per one meter of a lane in that section.

Figure 1 depicts an idealized relationship between *V* and *K*. When the road is not crowded, the highest speed is attained regardless of the level of *K*. But as the road gets crowded, the speed starts to decline. The graphs of the various specialized functions estimated in the literature approximate the downward sloping portion of this "true" *K*–*V* curve of this relationship.

[Insert Figure 1]

The functional specifications that appeared in the literature are listed below.

Greenshield (1935) developed a macroscopic stream model, in which density and speed are negatively linearly related as follow: (hereafter, the S model):

$$V = V^f \cdot \left[1 - \frac{K}{K^j} \right] \qquad \text{[S model]} \qquad (1)$$

Where V^f is the *free-flow speed* attained when the K is zero, while K^j is the value of K of that attains $V = 0$, which implies that K^j is the jam density (i.e., the maximum value of that K). The speed–density linearity relationship of S model has gradient V^f / K^j [1].

[1] These are single-regime models from the viewpoint of the congestion level of vehicles. Each model can also be derived from a microscopic approach that focuses on describing the detailed manner in which one vehicle follows another. The several studies in which driver behavior in another following car is modeled are typically referred to as car-following models of vehicular traffic

Greenberg (1959) assumed a logarithmic relationship between speed and density. He proposed the following model (hereafter, the B model):

$$V = V^c \cdot \ln\left[\frac{K^j}{K}\right], \qquad \text{[B model]} \qquad (2)$$

where V^c is the *critical speed* at the maximum traffic capacity, which is corresponding to $Q = Q^c$ in the quadrant IV of figure 1. When density K approaches zero, the speed V diverges to infinity. Thus, a disadvantage of this model is its inability to predict speeds at lower densities.

Underwood (1961) proposed the following exponential model (hereafter, the U model):

$$V = V^f \exp\cdot\left[-\frac{K}{K^c}\right], \qquad \text{[U model]} \qquad (3)$$

where K^c is the critical density corresponding to the maximum traffic capacity. The main drawback of this model is that speed becomes zero only when density reaches infinity. Hence, this model cannot be used for predicting speeds at high densities. Drake et al. (1967) proposed a similar model in the form of the half bell-shaped curve model (hereafter, the D model):

$$V = V^f \exp\cdot\left[-0.5\left(\frac{K}{K^c}\right)^2\right]\cdot \qquad \text{[D model]} \qquad (4)$$

Regression analysis is frequently used to examine the validity of these models. The right-hand sides of the traditional equations above characterize the deterministic functional form of the speed–density relationship. Assuming that V^f, V^c, K^j and K^c have unique values, the regression models corresponding to the equations (1), (2), (3) and (4) are as follows:

$$V_i = \begin{cases} a^S + b^S K_i + u_i \\ a^B + b^B \ln K_i + u_i \end{cases} \quad \text{and} \quad \ln V_i = \begin{cases} a^U + b^U K_i + u_i \\ a^D + b^D K_i^2 + u_i \end{cases} \qquad (5)$$

where V_i is the speed and K_i is the traffic density in road section i, the parameters of each

(Gazis et al. 1961). In the car-following model, by formulating the acceleration of each following vehicle with the leading vehicle, interrelationships between levels of speed–density states are derived. The acceleration of following vehicles is represented by a nonlinear differential equation in which the variables are the speeds of the following vehicles and their headway, as measured by, for example, distances between vehicles. The model generates the various speed–density functions referred to above in the form of the combinations of values taken by the exponents on the variables.

model are defined as $a^S = V^f$, $b^S = -V^f / K^j$, $a^B = -V^c \ln K^j$, $b^B = -V^c$, $a^U = \ln V^f$, $b^U = -1/K^c$, $a^D = \ln V^f$ and $b^D = -1/2K^{c^2}$, and u_i is a disturbance term. In each simple linear regression model, it is expected that the sign of gradient: b^S, b^B, b^U and b^D, are negative. In other speed–density models, such as those of Drew (1968) and Gazis et al. (1961), nonlinear functional forms are used.

3. The Empirical Model

In this section, we apply the improved empirical model of the speed–density relationship by using time-series cross-sectional data. In equation (5), with regard to the dependent and independent variables, we use the following notation:

$$y_{it} = \begin{cases} V_{it}, \text{ if a modle is S or B type} \\ \ln V_{it}, \text{ if a modle is U or D type} \end{cases}$$

$$x_{it} = \begin{cases} K_{it}, \text{ if a modle is S or U type} \\ \ln K_{it}, \text{ if a modle is B type} \\ K_{it}^2, \text{ if a modle is D type} \end{cases}, \quad (6)$$

where y_{it} is the dependent variable corresponding to speed and x_{it} is the independent variable corresponding to density on road section *i* in time period *t*. For each section, y_{it} and x_{it} are aggregated variables per hour. We observed three time intervals: 0700–0800 hours $(t = 1)$, 1300–1400 hours $(t = 2)$ and 1700–1800 hours $(t = 3)$.

We assume that in the speed–density relationship there are time-constant variables for section *i* and a time effect for period *t*. The speed–density relationship model with fixed unit, time and partial time effects is as follow:

$$y_{it} = \alpha_i + \beta x_{it} + \tau_2 D_{i2} + \tau_3 D_{i3} + \theta_2^1 D_{i2} DIR_i + \theta_3^1 D_{i3} DIR_i + \theta_2^2 D_{i2} SIG_i + \theta_3^2 D_{i3} SIG_i + u_{it}, \quad (7)$$

where the speed variable y_{it} and the density variable x_{it} have already been defined in the context of (6), α_i is a fixed effect for the *i* th section, τ_2 and τ_3 are time effects for

1300–1400 hours and 1700–1800 hours, respectively, D_{i2} and D_{i3} are time dummies for 1300–1400 hours and 1700–1800 hours, respectively, $\theta_2^1, \theta_3^1, \theta_2^2$ and θ_3^2 are partial time effects, DIR_i is a dummy variable for direction, SIG_i represents the density of traffic signals on section i and u_{it} is well-behaved disturbance term. DIR_i and SIG_i are time-constant variables. The terms of product in time-constant variables and time periods dummy variables control the partial time effects.

Each road section as a cross-section observation unit has a spatial linkage to other sections. Assuming that unobservable factors in each road section exist and have spatial autocorrelation, another disturbance term is as follow

$$u_{it} = \lambda \sum_{j=1}^{n} W_{ij} u_{jt} + \varepsilon_{it}, \tag{8}$$

where λ is a scalar parameter, which is typically referred to as the spatial autoregressive parameter, u_{it} denotes disturbance terms comprising a spatially autocorrelated disturbance term, W_{ij}, which is known, and the element of the spatial weight matrix, ε_{it}, which is the error term. We test the model specification later section. If spatial autocorrelation is founded, we also estimate the equation (8) by the method of Kelejian and Prucha (1999). The details of estimation procedures are noted in Appendix 1 and 2.

4. Data

We can now estimate the models of the speed–density relationship using spatial panel data. In this research, we focus not on highway traffic but on general road traffic in the twenty-three special wards of Tokyo. To understand the traffic stream in the entire urban area, we consider a variety of routes as our sample for analysis.

We use data on the traffic flow of vehicles at points of intersection on main trunk roads. The intersection traffic data are aggregated by the Metropolitan Police Department (MPD) based on

the original statistical reports *Traffic Statistics*, which reports observed vehicle inflows (and outflows) per hour to (and from) intersections aggregated to cover the interval from 0700 to 1900 hours. The traffic density on a particular section of road is defined as the ratio of aggregated traffic flow per hour on that section to the distance covered by that section. The data relate to December 13 and 14, 2005.

Data on vehicular speeds are based on figures from *The Metropolitan Police Department Traffic Yearbook* reported by the MPD. These statistics records journey time and speed from a particular intersection to another intersection between 0700–0800 hours, 1300–1400 hours and 1700–1800 hours. The routes on which traffic is observed comprise five loop routes and 15 radial routes. Within the area covered by these intersections (the intra-intersection) are 191 road sections running in both inner (to center) and outer (to suburb) directions.

Journey times are calculated from the *Database of Journey Time Statistics* collected by the MPD's traffic control system. A vehicle's (overall) journey speed on a section of road is defined as the distance of the section divided by the journey time.

To conduct our analysis, we matched the sections of the intra-intersection on which traffic flow data per hour was recorded in the MPD's *Traffic Statistics* to the sections on which journey times were recorded. The journey time recorded in the MPD's *Traffic Yearbook* covers three time intervals: 0700–0800 hours, 1300–1400 hours and 1700–1800 hours. The traffic flow data were made to correspond to these time intervals. The matched data cover three loop routes and 15 radial routes. Table 1 lists the names of these routes, the number of road sections included in each route and its total distance. The total number of sections on all routes is 97. For example, the nine sections in L1, Kanjo-hachi-gosen, total 26.5 km in length. Figure 2 maps the routes and intersections covering the twenty-three special wards of Tokyo.

[Insert Table 1]

[Insert Figure 2]

For illustration, Table 2 reports detailed data on each section in L1, Kanjo-hachi-gosen. Section 1 runs from Otorii to Minamikamata. This 1.8 km stretch has 12 sets of traffic lights. The inner direction runs from Minamikamata to Otorii and the outer direction runs from Otorii to Minamikamata. We have data covering the three time intervals mentioned above and three directions per section.

[Insert Table 2]

Table 3 reports descriptive statistics for the 97 routes over three time intervals and in two directions, which implies a total sample size of $582 = 97 \times 3 \times 2$. In inner directions (loop routes) and in directions to the center (radial routes), vehicle speed is fastest in the morning. Density does not vary much on these routes. The density on radial routes exceeds that on loop routes. In outer directions (loop routes) and in directions to suburbs (radial routes), vehicle speed is lowest in the morning. *DIR* is a dummy variable for direction and *SIG* is the number of traffic lights on the length of the corresponding intra-intersection: the density of signals. Both *DIR* and *SIG* are time-constant variables. We can test whether the effects of these time-constant variables change over time by using the cross products of time effects.

[Insert Table 3]

The data on the sections that connect within the intersection and the linkages between them

depend on the travelling directions. Figure 3 shows that L1, Kanjo-hachi-gosen (sections 1 and 2) intersects with R1, the Dai-ichi-keihin route (sections 30 and 31) within the Minamikamata intersection (intersection *a*). A vehicle that leaves Higashiyaguchi (intersection *b*) joins section 1 and section 30 at intersection *a* in the inner direction. Thus, section 2 in the inner direction is contiguous with sections 1 and 30. However, section 2 in the outer direction is not contiguous with either section 1, section 30 or section 31 because it runs in the opposite direction. Table 4 reports contiguity in each section and uses a code of unity to denote a section that is contiguous with another section by its direction, and uses a zero otherwise. This definition yields the contiguity matrix $\{c_{ij}\}$. The elements of the standardized spatial weight matrix, whose rows each sum to unity, are defined as $W_{ij} = c_{ij} \Big/ \sum_j c_{ij}$ for $i, j = 1, \cdots, n$.

[Insert Table 4]

[Insert Figure 3]

5. Testing and Estimation Results

5.1. Model Specification

To choose our preferred speed–density model, we perform specification tests as follows:

- $H_0^1 : \alpha_i = \alpha$ (with $\lambda = 0$). The null hypothesis is that the unit-specific term is constant for all i under the assumption that there is no spatial autocorrelation. We compare our OLS results on the pooled data based on incorporating a common constant term and dummy variables with the fixed effects panel data model. (Group effect *F*-test.)
- $H_0^2 : \mathrm{Cov}(\boldsymbol{\alpha}, \mathbf{X}) \neq 0$ (with $\lambda = 0$). The null hypothesis is that $\boldsymbol{\alpha}$ and $\mathbf{X}$ are uncorrelated under the assumption that there is no spatial autocorrelation, where $\mathbf{X}$ is explanation variable matrix. This specification test was devised by Hausman (1978) based on a

comparison of the fixed- and random-effects estimators.

- H_0^3: There is no spatial autocorrelation. We employ Moran's *I*-test with fixed effects. Moran's *I* is defined as $MI = \mathbf{e}'\overline{\mathbf{W}}\mathbf{e}/\mathbf{e}'\mathbf{e}$, where $\mathbf{e}$ is the pooled OLS residual vector. As shown by Cliff and Ord (1973), the asymptotic distribution for the statistic is standard normal: $SMI = (MI - E(MI))/V(MI)^{1/2} \sim N(0,1)$, where *SMI* denotes the standardized Moran's *I* test.
- $H_0^4: \lambda = 0$ (with $\alpha_i \neq \alpha$ and α_i as the fixed effect). Alternative Lagrange Multiplier testing procedures for the null hypothesis of no spatial error dependence are presented by Anselin (1988) and Baltagi *et al*. (2003). The test statistic is distributed as chi-squared with one degree of freedom, with 5% and 1% critical values of 3.84 and 6.63, respectively.
- $H_0^5: \sigma_\alpha^2 = 0$ (with $\lambda \neq 0$). Assuming the possible existence of spatial correlation, we test whether the variance of α_i is zero for the randomness of α_i (Baltagi *et al*. 2003, 2008). The test statistic is asymptotically distributed as standard normal.

5.2. Estimation Results

Based on the estimation results for equation (7), Table 5 reports the H_0^1, H_0^2, H_0^3 and H_0^4 test results for the S, B, U and D type speed–density models. Similar results were obtained for all four models. The test for group effects examines whether there are section-specific fixed effects. The OLS fixed-effects model incorporating dummy variables outperforms the OLS regression based on pooled data because the *p*-value is sufficiently small. The *p*-value for the Hausman test for fixed and random effects is sufficiently small. This suggests that the fixed-effects model is preferable to the random-effects model conditional on $\lambda = 0$. Given the *SMI*, the hypothesis that spatial correlation does not exists in the model is rejected. However, what alternative hypothesis of Moran's *I* test is acceptable is unclear. Assuming that fixed effects exist, the null hypothesis $\lambda = 0$ is rejected and the alternative hypothesis $\lambda \neq 0$ is

accepted.

[Insert Table 5]

Based on these test results, we estimate (7) with (8) treating α_i as a fixed effect. Using the residual from the fixed-effects regression model without spatial autocorrelation, we solve the generalized moments estimator to estimate λ (see Apendix). Both sides of equation (7) are multiplied by a Cochrane–Orcutt type weight to obtain feasible generalized least squared (FGLS) estimates .

Estimation results from the S, B, U and D speed–density models are reported in Tables 6, 7, 8 and 9, respectively.

[Insert Table 6 and 7]

[Insert Table 8 and 9]

Table 6 reports the estimation results from the S model, in which the dependent variable is $y = V$ and the density variable is $x = K$. Column I reports the FGLS estimates from the fixed-effects model with spatial error correlation, which corresponds to equation (A8) in Appendix 2. The parameter of density is negative and significant. The time effect is also negative. In particular, vehicle speeds are significantly lower (by about 4.874 km per hour) during evenings, compared with mornings, other circumstances being equal. The estimated coefficients of D_2DIR and D_3DIR show the effect of differences in the direction of the traffic flow. Vehicles travel faster out to suburbs than into the center (inner direction). The estimated coefficients of D_2SIG and D_3SIG show the effect of signal density in each time interval. The

greater is the number of traffic lights, the lower are vehicle speeds.

Column II of Table 6 reports results from the fixed-effects model with unit and time effects but without spatial autocorrelation. When $\lambda = 0$ is assumed, the estimated coefficients are quite large. Columns II and III report the estimation results from the fixed-effects model with unit effects but without time and partial time effects. The estimated coefficients of density K are too large. Omitting the time variables may have caused a bias. Column V in Table 6 reports the OLS estimates from pooling the data. When unit effects are ignored, the coefficient of density becomes insignificant.

Table 7 reports the estimation results from the Greenberg model, in which the dependent variable is $y = V$ and the density variable is $x = \ln K$. Table 8 reports the estimation results from the Underwood model, in which the dependent variable is $y = \ln V$ and the density variable is $x = K$. Table 9 reports the estimation results from the Drake model, in which the dependent variable is $y = \ln V$ and the density variable is $x = K^2$. For all models, the coefficients of D_3, D_2DIR, D_3DIR and D_2SIG are significant in column I, which reports the fixed-effects model with unit and time effects and spatial autocorrelation. Omitting the unit and time effects seems to cause a bias. The U and D models fit the data better than do the S and B models. However, the coefficient of density in the D model (see column I of Table 9) is not significant at the 5% level. Our empirical results indicate that the U model outperforms the other models in goodness of fit. This is consistent with Suzuki *et al*. (2006), who find that the exponential model is preferable in analyzing national road route 4 in Japan.

5.3. Critical Density and Critical Speed

The estimated fixed-effects models with unit and time effects and spatial autocorrelation have the following theoretical parameter values (in the context of $\hat{y}_{it} = \hat{\alpha}_{it} + \hat{\beta} x_{it}$):

$$\hat{\hat{\alpha}}_{it} = \begin{cases} \hat{\alpha}_i & t = 1 \\ \hat{\alpha}_i + \hat{\tau}_2 + \hat{\theta}_2^1 + \hat{\theta}_2^2 SIG_i & t = 2 \\ \hat{\alpha}_i + \hat{\tau}_3 + \hat{\theta}_3^1 + \hat{\theta}_3^2 SIG_i & t = 3 \end{cases}$$

if the direction is outer / to suburb and

$$\hat{\hat{\alpha}}_{jt} = \begin{cases} \hat{\alpha}_j & t = 1 \\ \hat{\alpha}_j + \hat{\tau}_2 + \hat{\theta}_2^2 SIG_j & t = 2 \\ \hat{\alpha}_j + \hat{\tau}_3 + \hat{\theta}_3^2 SIG_j & t = 3 \end{cases}$$

if the direction is inner / to center. We use equation (5) to determine the critical densities and critical speeds in the S, B, U and D types. Table 10 reports these theoretical values for each model. If the function of speed–density relationship is specified as $V = V(K)$, the critical density corresponding to the maximum traffic flow satisfies $V(K^c) + K^c V'(K^c) = 0$ and $V^c = V(K^c)$. In the S model, the critical density and critical speed depend on the road section and time variations. In the B model, the critical density depends on the road section and time variations, but critical speed has a unique value. In the U and D models, critical density has a unique value, but critical speed depends on the road section and time variations.

[Insert Table 10]

Table 11 reports average measured critical density values. The B model's critical density exceeds those of the other models. In Figures 4 and 5, the speed–density curve for the B model is slightly curved. The critical densities of the U and D models are intermediate values. The B model has the lowest critical speed (Table 12). The critical speed for inner direction of loop routes at 0700–0800 hours exceeds all other critical speeds. It is similar for radial routes. Figure 6 shows the speed–density relationship for the U model for each time interval. In the inner (to center) direction, we expect the critical speed to increase quickly to reach the critical density

$(K^c = 2.3)$, compared with other morning time intervals.

[Insert Table 11]

[Insert Table 12]

[Insert Figure 4 and 5]

[Insert Figure 6]

6. Conclusion

We analyzed aggregated road network linkage data to understand the speed–density relationship in an entire urban area by using spatial panel data aggregated by each route. Because we found evidence of spatial autocorrelation in each road section, to obtain efficient estimates, we used a weighted regression model with spatial autocorrelation. In the context of the classical speed–density relationship, we compared functional forms and such unique regression model parameters as the critical density and the critical speed.

We obtained the following findings.

- Unobserved unit effects seemed significant on all routes. Moreover, we found evidence of spatial correlation among contiguous routes in our data. When disregarding the unit effects and time effects, the coefficient of density became insignificant.
- When using feasible generalized least squares estimation with a generalized moments estimator, the parameter of density was negative and significant in the Greenshield (S), Greenberg (B) and Underwood (U) models. In the Drake (D) model, the estimated coefficient of density was not significant at the 5% level.
- The critical densities of the U and D models are in between those of the B and S models, with the former being the highest. The critical speed on inner loop routes is highest at

0700–0800 hours. It is similar on radial routes.

Appendix 1. A Panel Model with Spatial Disturbance

The speed–density regression model with two-way fixed effects, partial time effects and spatial autocorrelation disturbance is given by:

$$y_{it} = \alpha_i + \beta x_{it} + \tau_t + \theta_t z_{it} + u_{it}, \quad u_{it} = \lambda \sum_{j=1}^{n} W_{ij} u_{jt} + \varepsilon_{it} \ (i = 1, \cdots, n, \ t = 1, \cdots, T), \tag{A1}$$

where α_i is the unobservable fixed unit effect, τ_t is the unobservable fixed time effect, z_{it} is the product of the time period dummy variable d_{it}^{s} corresponding to the time effect, where $d_{is}^{t} = 1$ if $s = t$, and the observable time-constant variables z_i; that is, $z_{it} = d_{it}^{t} z_i$. In addition, u_{it} denotes disturbance terms comprising a spatially autocorrelated disturbance term, W_{ij}, which is known, and the element of the spatial weight matrix, ε_{it}, which is the error term. The parameters β, $\boldsymbol{\theta}$ and λ are unknown. We assume that ε_{it} is an independent and identically distributed error term that is well behaved: $E(\varepsilon_{it}\varepsilon_{js}) = 0$ for $i \neq j$ and $t \neq s$.

Equation (A1) is the panel regression model with fixed effects and a spatially autocorrelated disturbance. The constant term in the speed–density linear equations (5) is allowed to differ according to time and road section. For example, in the S model, the free speed, V_f, takes a specific value by observed time and section. We can estimate the differences in the partial effects from the time-constant variables relative to a base time period, such as $t = 1$. In particular, we can test whether the effects of the time-constant variables change over time. In estimation, a time dummy variable for base period is excluded to avoid perfect collinearity, and we set the first time period effect τ_1 to zero.

By stacking the units incorporated in (A1), for each time period, we have:

$$\mathbf{y}_t = \boldsymbol{\alpha} + \beta \mathbf{x}_t + \tau_t + \theta_t z_{it} + \mathbf{u}_t, \tag{A2}$$

$$\mathbf{u}_t = \lambda \mathbf{W} \mathbf{u}_t + \boldsymbol{\varepsilon}_t, \tag{A3}$$

where $\mathbf{y}_t = (y_{1t}, \cdots, y_{nt})'$ is an $n \times 1$ vector, as is $\boldsymbol{\alpha} = (\alpha_1, \cdots, \alpha_n)'$, with $\mathbf{x}_t$ and $\mathbf{u}_t$ being similarly defined $n \times 1$ vectors and $\mathbf{W}$ being the time-constant spatial weight matrix. One can rewrite the spatial autoregressive term (A3) as $\mathbf{u}_t = (\mathbf{I}_{(n)} - \lambda \mathbf{W})^{-1} \boldsymbol{\varepsilon}_t = \mathbf{B}^{-1} \boldsymbol{\varepsilon}_t$, where $\mathbf{B} = \mathbf{I}_{(n)} - \lambda \mathbf{W}$ and $\mathbf{I}_{(n)}$ is an $n \times n$ identity matrix. Stacking (A2) and (A3) across time periods yields:

$$\mathbf{y} = (\boldsymbol{\iota}_{(T)} \otimes \mathbf{I}_{(n)})\boldsymbol{\alpha} + \mathbf{x}\beta + (\widetilde{\mathbf{I}}_{(T)} \otimes \boldsymbol{\iota}_{(n)})\boldsymbol{\tau} + (\widetilde{\mathbf{I}}_{(T)} \otimes \mathbf{z})\boldsymbol{\theta} + \mathbf{u}, \tag{A4}$$

$$\mathbf{u} = (\mathbf{I}_{(T)} \otimes \mathbf{B}^{-1})\boldsymbol{\varepsilon}, \tag{A5}$$

where $\mathbf{y} = [\mathbf{y}_1', \cdots \mathbf{y}_T']'$ is an $nT \times 1$ vector, and $\mathbf{x}$, $\mathbf{u}$ and $\boldsymbol{\varepsilon}$ are similarly defined. In addition, $\boldsymbol{\iota}_{(T)}$ and $(\boldsymbol{\iota}_{(n)})$ are vectors of ones of dimension T and n, respectively. $\mathbf{I}_{(T)}$ is an identity matrix of dimension T, $\otimes$ denotes the Kronecker product, $\widetilde{\mathbf{I}}_{(T)}$ is a $T \times (T-1)$ matrix that excludes the first row of a $T \times T$ identity matrix to avoid perfect collinearity; that is,

$$\widetilde{\mathbf{I}}_{(T)} = \underbrace{\begin{pmatrix} 0 & 0 & \cdots & 0 \\ 1 & 0 & \cdots & 0 \\ 0 & 1 & & 0 \\ \vdots & & \ddots & \\ 0 & 0 & & 1 \end{pmatrix}}_{T-1 \text{ column}}.$$

Further, $\mathbf{z} = (z_1, \cdots, z_n)'$, $\boldsymbol{\tau} = (\tau_2, \cdots, \tau_T)'$ and $\boldsymbol{\theta} = (\theta_2, \cdots, \theta_T)'$. The matrix $\boldsymbol{\iota}_{(T)} \otimes \mathbf{I}_{(n)}$ is of dimension $nT \times n$. The matrices $(\widetilde{\mathbf{I}}_{(T)} \otimes \boldsymbol{\iota}_{(n)})$ and $(\widetilde{\mathbf{I}}_{(T)} \otimes \mathbf{z})$ are of dimension $nT \times (T-1)$. The matrix $\mathbf{I}_{(T)} \otimes \mathbf{B}^{-1}$ is of dimension $nT \times nT$.

The variance of (A5), $E(\mathbf{u}\mathbf{u}')$, has, in general, a nonspherical structure, which is a function of the spatial autoregressive parameter λ, the spatial weight matrix $\mathbf{W}$ and the true variance of $\boldsymbol{\varepsilon}$. Because $\mathbf{W}$ is known, $E(\mathbf{u}\mathbf{u}')$ is known up to λ and the true variance of $\boldsymbol{\varepsilon}$, which we estimate.

We assume that λ is known as λ^* and define $\mathbf{B}^* = \mathbf{I}_{(n)} - \lambda^* \mathbf{W}$. To address

heteroskedasticity in the disturbance, we can premultiply the model in (A4) as follows:

$$\left(\mathbf{I}_{(T)} \otimes \mathbf{B}^{*}\right)\mathbf{y} = \left(\mathbf{I}_{(T)} \otimes \mathbf{B}^{*}\right)\mathbf{X}\boldsymbol{\Gamma} + \boldsymbol{\varepsilon}, \tag{A6}$$

where $X = \left[\boldsymbol{\iota}_{(T)} \otimes \mathbf{I}_{(n)},\ \mathbf{x},\ \widetilde{\mathbf{I}}_{(T)} \otimes \boldsymbol{\iota}_{(n)},\ \widetilde{\mathbf{I}}_{(T)} \otimes \mathbf{z}\right]$ is an $nT \times (n + 2T - 1)$ matrix and $\boldsymbol{\Gamma} = \left[\boldsymbol{\alpha}', \beta, \boldsymbol{\tau}', \boldsymbol{\theta}'\right]'$ is an $(n + 2T - 1) \times 1$ vector. If the weighted regression model (A6) has a well-behaved disturbance, one can apply the generalized least squares method.

Appendix 2. The Generalized Moments Estimator and the Feasible Generalized Least Squares Method

Kelejian and Prucha (1999) developed a moments estimator of the parameter λ in a cross-sectional setting $(T = 1)$. We extend their approach by applying their estimator to our panel data model with a two-way fixed effects. Consider the following three moment conditions:

$$E\left(\frac{1}{nT}\boldsymbol{\varepsilon}'\boldsymbol{\varepsilon}\right) = \sigma^2,$$

$$E\left(\frac{1}{nT}\boldsymbol{\varepsilon}'\overline{\mathbf{W}}'\overline{\mathbf{W}}\boldsymbol{\varepsilon}\right) = \frac{1}{n}\sigma^2 \operatorname{tr}(\mathbf{W}'\mathbf{W}),$$

$$E\left(\frac{1}{nT}\boldsymbol{\varepsilon}'\overline{\mathbf{W}}'\boldsymbol{\varepsilon}\right) = 0,$$

where σ^2 is the true variance of ε_{it}, $\overline{\mathbf{W}} = \mathbf{I}_{(T)} \otimes \mathbf{W}$ and $\operatorname{tr}(\cdot)$ denotes the trace of a matrix. Noting that $\overline{\mathbf{u}} = \overline{\mathbf{W}}\mathbf{u}$ and $\boldsymbol{\varepsilon} = \mathbf{u} - \lambda\overline{\mathbf{u}}$, the three-equation system implies:

$$\frac{2}{nT}E(\mathbf{u}'\overline{\mathbf{u}})\cdot\lambda - \frac{1}{nT}E(\overline{\mathbf{u}}'\overline{\mathbf{u}})\cdot\lambda^2 + \sigma^2 = \frac{1}{nT}E(\mathbf{u}'\mathbf{u})$$

$$\frac{2}{nT}E(\overline{\mathbf{u}}'\overline{\mathbf{W}}\mathbf{u})\cdot\lambda - \frac{1}{nT}E(\overline{\mathbf{u}}'\overline{\mathbf{W}}'\overline{\mathbf{W}}\,\overline{\mathbf{u}})\cdot\lambda^2 + \frac{1}{n}\operatorname{tr}(\mathbf{W}'\mathbf{W})\cdot\sigma^2 = \frac{1}{nT}E(\overline{\mathbf{u}}'\overline{\mathbf{W}}\mathbf{u})$$

$$\frac{1}{nT}E(\overline{\mathbf{u}}'\overline{\mathbf{W}}'\mathbf{u} + \overline{\mathbf{u}}'\overline{\mathbf{W}}\,\mathbf{u})\cdot\lambda - \frac{1}{nT}E(\overline{\mathbf{u}}'\overline{\mathbf{W}}'\overline{\mathbf{u}})\cdot\lambda^2 = \frac{1}{nT}E(\overline{\mathbf{u}}'\overline{\mathbf{W}}'\mathbf{u})$$

.

Now consider the following analogue to the moments condition in terms of sample moments based on the residual vector $\mathbf{e}$ from the two-way fixed effects regression implied by equation

(A4). Noting that $\bar{\mathbf{e}} = \overline{\mathbf{W}}\mathbf{e}$, the three-equation system can be rewritten in matrix form as:

$$\begin{bmatrix} \frac{2}{nT}\mathbf{e}'\bar{\mathbf{e}} & -\frac{1}{nT}\bar{\mathbf{e}}'\bar{\mathbf{e}} & 1 \\ \frac{2}{nT}\bar{\mathbf{e}}'\overline{\mathbf{W}}\mathbf{e} & -\frac{1}{nT}\bar{\mathbf{e}}'\overline{\mathbf{W}}'\overline{\mathbf{W}}\bar{\mathbf{e}} & \frac{1}{n}\mathrm{tr}\left(\mathbf{W}'\mathbf{W}\right) \\ \frac{1}{nT}\bar{\mathbf{e}}'\left(\overline{\mathbf{W}}'\mathbf{e}+\bar{\mathbf{e}}\right) & -\frac{1}{nT}\bar{\mathbf{e}}'\overline{\mathbf{W}}'\bar{\mathbf{e}} & 0 \end{bmatrix}\begin{bmatrix} \lambda \\ \lambda^2 \\ \sigma^2 \end{bmatrix} - \begin{bmatrix} \frac{1}{nT}\mathbf{e}'\mathbf{e} \\ \frac{1}{nT}\bar{\mathbf{e}}'\overline{\mathbf{W}}\mathbf{e} \\ \frac{1}{nT}\bar{\mathbf{e}}\,\overline{\mathbf{W}}\,\mathbf{e} \end{bmatrix} = \xi\left(\lambda,\sigma^2\right) \qquad \text{(A7)}$$

,

where $\xi(\lambda,\sigma^2)$ is the error vector associated with a sample of statistical realizations. The nonlinear least squares estimator $\left(\hat{\lambda},\hat{\sigma}^2\right)$ minimizes $\xi(\lambda,\sigma^2)'\xi(\lambda,\sigma^2)$ and is consistent for sufficiently large n. We define $\hat{\mathbf{B}} = \mathbf{I}_{(n)} - \hat{\lambda}\mathbf{W}$ as estimated weight matrix to compute (A6). These estimates yield $\left(\mathbf{I}_{(T)} \otimes \hat{\mathbf{B}}\right)$, which can be substituted into equation (A6). Then, we have the following FGLS estimator:

$$\hat{\mathbf{\Gamma}} = \left[\mathbf{X}'\left(\mathbf{I}_{(T)} \otimes \hat{\mathbf{B}}'\hat{\mathbf{B}}\right)\mathbf{X}\right]^{-1}\mathbf{X}'\left(\mathbf{I}_{(T)} \otimes \hat{\mathbf{B}}'\hat{\mathbf{B}}\right)\mathbf{y}\,, \qquad \text{(A8)}$$

where $\hat{\mathbf{\Gamma}} = \left[\hat{\boldsymbol{\alpha}}', \hat{\beta}, \hat{\boldsymbol{\tau}}', \hat{\boldsymbol{\theta}}'\right]'$, which comprises the fixed unit effects, the marginal effect of traffic density, the fixed time effects and the partial time effects of the time-constant variable.

References

1). Anselin, L., (1988), *Spatial Econometrics: Methods and Models*, Kluwer Academic Pub.

2). Baltagi, B. H., Song, S. H. and W. Koh, (2003), "Testing Panel Data Regression Models with Spatial Error Correlation," *Journal of Econometrics*, 117(1), pp. 123–150.

3). Baltagi, B. H., Song, S. H., W., Koh and B.C. Jung, (2007), "Testing for Serial Correlation, Spatial Autocorrelation and Random Effects using Panel Data," *Journal of Econometrics*, 140, pp. 5–51.

4). Baltagi, B. H. and L. Liu, (2008), "Testing for Random Effects and Spatial Lag Dependence in Panel Data Models," *Statistics and Probability Letters*, 78(18), pp. 3304–3306.

5). Baltagi, B. H., Song, S. H. and J. H. Kwon, (2009), "Testing for Heteroskedasticity and Spatial Correlation in a Random Effects Panel Data Model," *Computational Statistics and Data Analysis*, 53(8), pp. 2897–2922.

6). Cascetta, E., (2009), *Transportation Systems Analysis*: *Models and Applications*, 2nd ed., Chapter 2, Springer.

7). Castillo, J. M. D. and F. G. Benitez, (1995), "On the Functional Form of the Speed–Density Relationship-I: General Theory," *Transportation Research Part B*: Methodological, 29, pp. 373–389.

8). Cliff, A. D. and J. K. Ord, (1973), *Spatial Autocorrelation, Vol. 5, Monographs in Spatial and Environmental Systems Analysis*, Pion, London.

9). Drake, J. S., Schofer, J. L. and A. D. May, (1967), "A Statistical Analysis of Speed Density Hypotheses," *Third International Symposium on the Theory of Traffic Flow Proceedings*, Elsevier North Holland, Inc., New York.

10). Drew, D. R., (1968), *Traffic Flow Theory and Control*, Chapter 12, McGraw-Hill Book

Company.

11). Kapoora, M., Kelejian, H. H. and I. R. Prucha, (2007), "Panel Data Models with Spatially Correlated Error Components," *Journal of Econometrics*, 140, pp. 97–130.

12). Kelejian, H. H. and I. R. Prucha, (1999), "A Generalized Moments Estimator for the Autoregressive Parameter in a Spatial Model," *International Economic Review*, 40, pp. 509–533.

13). Gazis, D.C., Herman, R. and R. W. Rothery, (1961), "Nonlinear Follow-the-Leader Models of Traffic Flow," *Operations Research*, INFORMS, pp. 545–567.

14). Greene, W. H., (2007), *Econometric Analysis*, 6th ed., Prentice Hall College.

15). Greenshield, B. D., (1935), "A Study of Traffic Capacity," *Highway Research Board Proceedings*, 14, pp. 448–477.

16). Greenberg, H., (1959), "An Analysis of Traffic Flow," *Operations Research*, 7, pp. 78–85.

17). Suzuki, S., Taniguchi, M. and T. Takagi, (2006), "Exponential Modeling of Road Traffic Flow," *The Society of Instrument and Control Engineers Tohoku Chapter Research Convention*, 230–15 (in Japanese).

18). Underwood, R. T., (1961), "Speed, Volume, and Density Relationships: Quality and Theory of Traffic Flow," *Yale Bureau of Highway Traffic*, pp. 141–188.

19). Wang, H., Li, J., Chen, Q. and D. Ni, (2009), "Speed–Density Relationship: From Deterministic to Stochastic," *Transportation Research Board Annual Meeting*, Paper #09–1527.

Table 1. Summary of observed routes

Name of routes	Number of sections included in route	Total distance [km]
Loop routes		
L1 Kanjo-hachi-gosen	9	26.5
L2 Kanjo-nana-gosen	10	55.4
L3 Yamate-dori	8	15.5
Radial routes		
R1 Dai-ichi-keihin	4	10.4
R2 Sakurada-dori and Dai-ni-keihin	7	14.4
R3 Aoyama-dori and Tamagawa-dori	7	12.8
R4 Shinjuku-dori and Kosyu-kaido	5	19.4
R5 Oume-kaido	5	14.9
R6 Shin-Oume-kaido	2	6.5
R7 Mejiro-dori	6	11.0
R8 Kasuga-dori and Kawagoe-kaido	3	10.0
R9 Hakusan-dori and Nakasendo	3	6.3
R10 Syowa-dori and Niko-kaido	5	11.6
R11 Edo-dori and Mito-kaido	5	9.6
R12 Kuramae-bashi-dori	5	10.1
R13 Keiyo-doro	5	8.6
R14 Kasaibashi-dori	5	7.5
R15 Harumi-dori	3	2.7
Total	97	253.2

note: Both ends of intersections name are as follows:

	Start (End)	End (Start)
L1	Otorii	Minamitanaka-2-chome
L2	Omorihigashi	Kasairinkaikoen
L3	Kitashinagawa-2-chome	Nakajuku
R1	Yatsuyamabashi	Rokugobashi
R2	Hibiya	Tamagawabashi
R3	Miyakezaka	Seta
R4	Sakuradamon	Chofusyomae
R5	Shinjukudaiguardnishi	Tanashicho-1-chome
R6	Nishiochiai-1-chome	Igusa-3-chome
R7	Kudanshita	Sangendera
R8	Ikebukuro-mutsumatarikkyo	Tosaibashi
R9	Nishisugamo	Funato
R10	Uenoekimae	Sujinbashi
R11	Marunouchi-1-chome	Kanamachi-3-chome
R12	Kuramae-1-chome	Ichikawabashi
R13	Ryogokubashi-nishizume	Yagochi
R14	Eitai-2-chome	Urayasubashi
R15	Iwaidabashi	Harumibashi-nishi

Table 2. Data of intersection included in L1: Kanjo-hachi-gosen

	Name of intersection	Distance [km]	Number of traffic light	Average speed [km/hour] 0700−0800 inner	0700−0800 outer	1300−1400 inner	1300−1400 outer	1700−1800 inner	1700−1800 outer
	Otorii								
section-1		1.8	12	15.8	20.4	15.0	14.2	16.1	10.7
	Minamikamata								
section-2		2.6	10	18.2	32.4	14.9	28.3	16.8	27.9
	Higashiyaguchi								
section-3		3.2	15	28.8	33.5	30.8	29.1	31.1	24.5
	Denenchofusyomae								
section-4		3.5	10	30.6	37.1	33.9	33.0	31.9	27.6
	Todorokihudoumae								
section-5		2.6	9	15.8	14.7	25.8	24.8	21.0	12.8
	Seta								
section-6		2.1	7	11.5	26.9	15.4	32.4	12.9	26.0
	Kanpachisetagaya								
section-7		4.0	12	20.7	25.5	25.4	20.7	24.0	12.6
	Kamitakaido-1chome								
section-8		4.1	20	10.1	26.9	21.9	18.7	20.7	14.8
	Shimendo								
section-9		2.6	15	18.0	15.4	21.3	13.5	20.0	13.2
	Minamitanaka-2chome								
	Total	26.5	110						
	Mean	2.9	12.2	18.8	25.9	22.7	23.9	21.6	18.9

Note: Data source is *The Metropolitan Police Department Traffic Yearbook* 2005 except number of traffic light, which is examined by *Google Map* (http://maps.google.co.jp/).

Table 3. Descriptive statistics: 97 routes, 3 time intervals and 2 directions

Variable	Routes	Directions	Time Zones	Mean	Std. Dev.	Min	Max	Number of Obs.
V (Speed)	Loop	Inner	7--8	25.90	5.80	14.70	37.10	27
			13--14	24.42	5.20	13.50	33.20	27
			17--18	19.96	6.29	10.70	30.30	27
		Outer	7--8	20.19	6.18	10.10	30.90	27
			13--14	23.66	5.73	14.80	33.90	27
			17--18	22.59	5.81	12.90	31.90	27
	Radial	To center	7--8	28.01	6.13	14.40	45.60	70
			13--14	23.05	4.42	14.00	32.10	70
			17--18	20.31	5.10	8.70	31.00	70
		To suburb	7--8	20.23	6.80	5.90	36.30	70
			13--14	22.42	5.25	10.80	33.70	70
			17--18	22.89	5.75	9.70	36.60	70
K (Density)	Loop	Inner	7--8	0.14	0.06	0.06	0.29	27
			13--14	0.16	0.07	0.05	0.33	27
			17--18	0.17	0.07	0.06	0.32	27
		Outer	7--8	0.16	0.07	0.06	0.32	27
			13--14	0.16	0.07	0.06	0.30	27
			17--18	0.17	0.07	0.07	0.32	27
	Radial	To center	7--8	0.24	0.15	0.07	0.86	70
			13--14	0.31	0.19	0.08	1.21	70
			17--18	0.35	0.26	0.10	1.94	70
		To suburb	7--8	0.35	0.21	0.07	1.09	70
			13--14	0.33	0.19	0.07	0.94	70
			17--18	0.34	0.20	0.07	1.11	70
DIR (Directions)						0	1	194
SIG (Density of Signals)				4.72	1.75	0.81	13.00	97

Note: *V* : average speed [km/hour], *K* : density [number of vehicles /meter, hour, lane], *DIR* : travel direction dummy variable as 1 if the section is outer direction (or direction to suburb), zero otherwise, *SIG* : density of signal [number of traffic light/distance]

Table 4. Spatial contiguity depending on directions (see figure 3)

		inner / to center				outer / to suburb			
		section-1	section-2	section-30	section-31	section-1	section-2	section-30	section-31
inner/to center	section-1	0	0	0	0	0	0	0	0
	section-2	1	0	1	0	0	0	0	1
	section-30	0	0	0	0	0	0	0	0
	section-31	1	0	1	0	0	1	0	0
outer / to suburb	section-1	0	0	1	0	0	1	0	1
	section-2	0	0	0	0	0	0	0	0
	section-30	1	0	0	0	0	1	0	1
	section-31	0	0	0	0	0	0	0	0

Table 5. Testing the fixed effects and spatial autocorrelation

	(1) Greenshield		(2) Greenberg		(3) Underwood		(4) Drake	
	statistics	*p*-value	statistics	*p*-value	statistics	*p*-value	statistics	*p*-value
H^1: Group Effect	5.699	[.000]	5.747	[.000]	5.193	[.000]	5.100	[.000]
H^2: Hausman Test	74.826	[.000]	76.923	[.000]	68.184	[.000]	65.385	[.000]
H^3: SMI	6.407	[.000]	6.422	[.000]	6.153	[.000]	6.134	[.000]
H^4: LM_λ	12.607	[.000]	12.655	[.000]	11.593	[.001]	11.539	[.001]

Table 6. Speed-density relationship (G Model: Geenshields): Dependent variable is $y = V$.

	I		II		III		IV		V	
	Coef.	p-value	Coef.	p-value	Coef.	p-value	Coef.	p-value	Coef.	p-value
const.	-		-		-		-		23.328	[.000]
K	−10.328	[.001]	−11.066	[.000]	−27.850	[.000]	−26.340	[.000]	−1.879	[.159]
D_2	−0.494	[.661]	−0.567	[.627]	-		-		-	
D_3	−4.874	[.000]	−4.887	[.000]	-		-		-	
D_2DIR	5.560	[.000]	5.761	[.000]	-		-		-	
D_3DIR	8.715	[.000]	8.766	[.000]	-		-		-	
D_2SIG	−0.593	[.006]	−0.598	[.007]	-		-		-	
D_3SIG	−0.302	[.182]	−0.288	[.190]	-		-		-	
FE (α)	Yes		Yes		Yes		Yes		-	
λ	0.383		-		0.498		-		-	
H^5: $\sigma_\alpha^2 = 0$	0.474	[.318]			0.293	[.385]				
R^2	0.800		0.757		0.765		0.669		0.003	

Table 7. Speed-density relationship (B Model: Greenberg): Dependent variable is $y = V$.

	I		II		III		IV		V	
	Coef.	P-value	Coef.	P-value	Coef.	P-value	Coef.	P-value	Coef.	P-value
const.	-		-		-		-		21.644	[.000]
ln K	−4.979	[.000]	−5.244	[.000]	−12.526	[.000]	−12.211	[.000]	−0.784	[.055]
D_2	−0.325	[.773]	−0.425	[.716]	-		-		-	
D_3	−4.642	[.000]	−4.659	[.000]	-		-		-	
D_2DIR	5.072	[.000]	5.246	[.000]	-		-		-	
D_3DIR	8.111	[.000]	8.128	[.000]	-		-		-	
D_2SIG	−0.531	[.014]	−0.527	[.017]	-		-		-	
D_3SIG	−0.225	[.320]	−0.203	[.352]	-		-		-	
FE (α)	Yes		Yes		Yes		Yes		-	
λ	0.382		-		0.465		-		-	
H^5: $\sigma_\alpha^2 = 0$	0.458	[.324]			0.266	[.395]				
R^2	0.801		0.759		0.774		0.697		0.006	

Table 8. Speed-density relationship (U Model: Underwood): Dependent variable is $y = \ln V$.

	I		II		III		IV		V	
	Coef.	P-value	Coef.	P-value	Coef.	P-value	Coef.	P-value	Coef.	P-value
const.	-		-		-		-		3.113	[.000]
K	−0.432	[.005]	−0.464	[.003]	−1.223	[.000]	−1.146	[.000]	−0.094	[.142]
D_2	0.012	[.834]	0.012	[.843]	-		-		-	
D_3	−0.201	[.001]	−0.205	[.001]	-		-		-	
D_2DIR	0.255	[.000]	0.266	[.000]	-		-		-	
D_3DIR	0.424	[.000]	0.418	[.000]	-		-		-	
D_2SIG	−0.028	[.009]	−0.029	[.008]	-		-		-	
D_3SIG	−0.018	[.110]	−0.015	[.164]	-		-		-	
FE (α)	Yes		Yes		Yes		Yes		-	
λ	0.453		-		0.520		-		-	
H^5: $\sigma_\alpha^2 = 0$	1.188	[.117]			0.927	[.177]				
R^2	0.927		0.739		0.922		0.653		0.004	

Table 9. Speed-density relationship (D Model: Drake): Dependent variable is $y = \ln V$.

	I		II		III		IV		IV	
	Coef.	P-value	Coef.	P-value	Coef.	P-value	Coef.	P-value	Coef.	P-value
const.	-		-		-		-		3.094	[.000]
K^2	−0.136	[.074]	−0.156	[.045]	−0.397	[.000]	−0.361	[.000]	−0.065	[.250]
D_2	0.004	[.946]	0.003	[.965]	-		-		-	
D_3	−0.227	[.000]	−0.229	[.000]	-		-		-	
D_2DIR	0.285	[.000]	0.290	[.000]	-		-		-	
D_3DIR	0.448	[.000]	0.448	[.000]	-		-		-	
D_2SIG	−0.031	[.004]	−0.031	[.004]	-		-		-	
D_3SIG	−0.017	[.139]	−0.016	[.148]	-		-		-	
FE (α)	Yes		Yes		Yes		Yes		-	
λ	0.404		-		0.561		-		-	
H^5: $\sigma_\alpha^2 = 0$	1.244	[.107]			0.967	[.167]				
R^2	0.917		0.735		0.901		0.620		0.002	

Table 10. Critical density and speed

Model	Critical Density: K^c	Critical Speed: V^c
S	$-\frac{1}{2}\frac{\hat{\hat{\alpha}}_{it}}{\hat{\beta}}$	$\frac{1}{2}\hat{\hat{\alpha}}_{it}$
B	$\exp\left[-\frac{\hat{\hat{\alpha}}_{it}}{\hat{\beta}}-1\right]$	$-\hat{\beta}$
U	$-\frac{1}{\hat{\beta}}$	$\exp\left[\hat{\hat{\alpha}}_{it}-1\right]$
D	$\sqrt{-\frac{1}{2\hat{\beta}}}$	$\exp\left[\hat{\hat{\alpha}}_{it}-\frac{1}{2}\right]$

Table 11. Measured critical density of average

		Inner / to center			Outer /to suburb		
Routes	Model	0700−0800	1300−1400	1700−1800	0700−0800	1300−1400	1700−1800
Loop $n = 27$	S	1.4	1.2	1.1	1.1	1.2	1.2
	B	16.6	9.5	5.3	5.9	9.2	9.5
	U	2.3					
	D	1.9					
Radial $n = 70$	S	1.5	1.3	1.2	1.2	1.3	1.3
	B	33.4	19.0	10.6	12.8	20.3	20.7
	U	2.3					
	D	1.9					

Table 12. Measured critical speed of average

		Inner / to center			Outer /to suburb		
Routes	Model	0700−0800	1300−1400	1700−1800	0700−0800	1300−1400	1700−1800
Loop $n = 27$	S	14.2	12.6	11.0	11.1	12.2	12.3
	B	5.0					
	U	10.5	9.3	7.9	7.9	9.1	9.0
	D	16.5	14.3	12.1	12.1	14.0	14.0
Radial $n = 70$	S	15.0	13.4	11.9	11.9	13.0	13.1
	B	5.0					
	U	11.3	10.0	8.5	8.4	9.6	9.6
	D	16.8	14.6	12.4	12.1	14.0	13.9

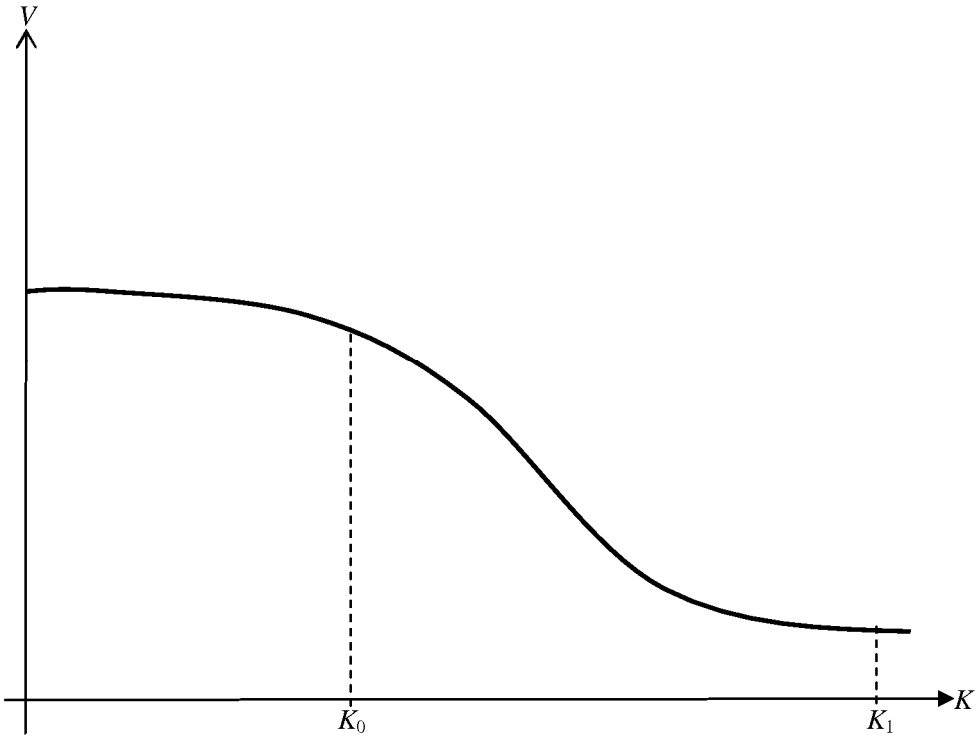

Figure 1. Idealized speed-density relationship

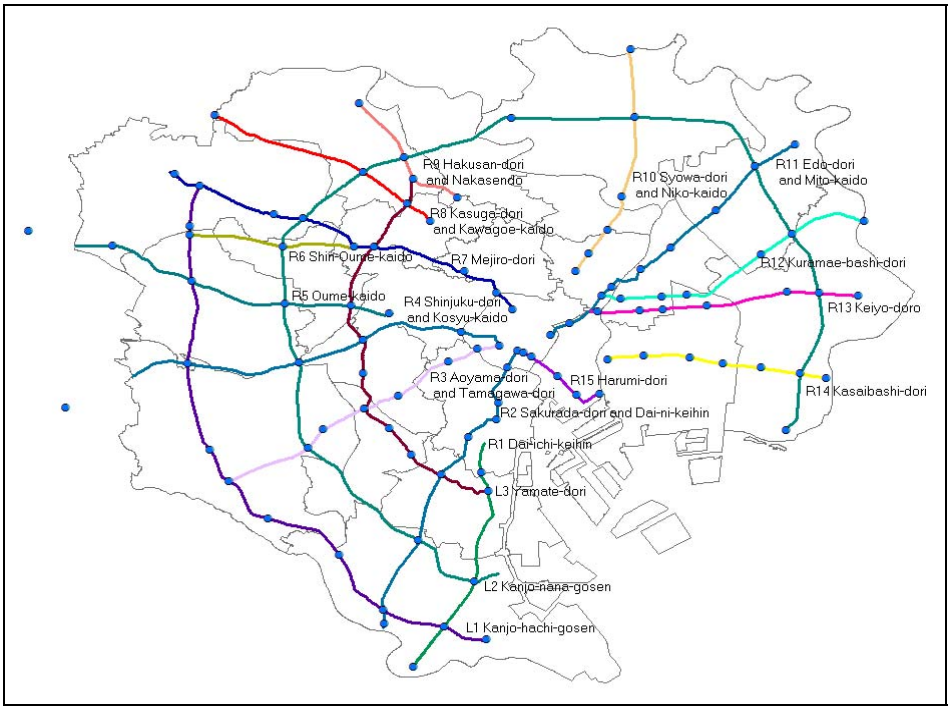

Figure 2. Observed routes and intersections

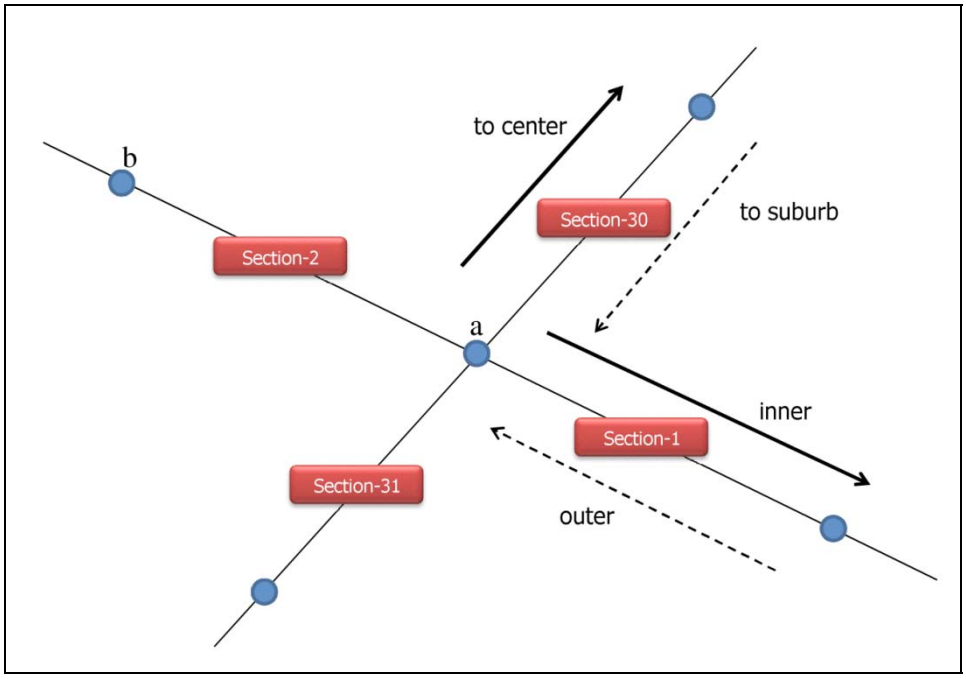

Figure 3. Spatial linkage

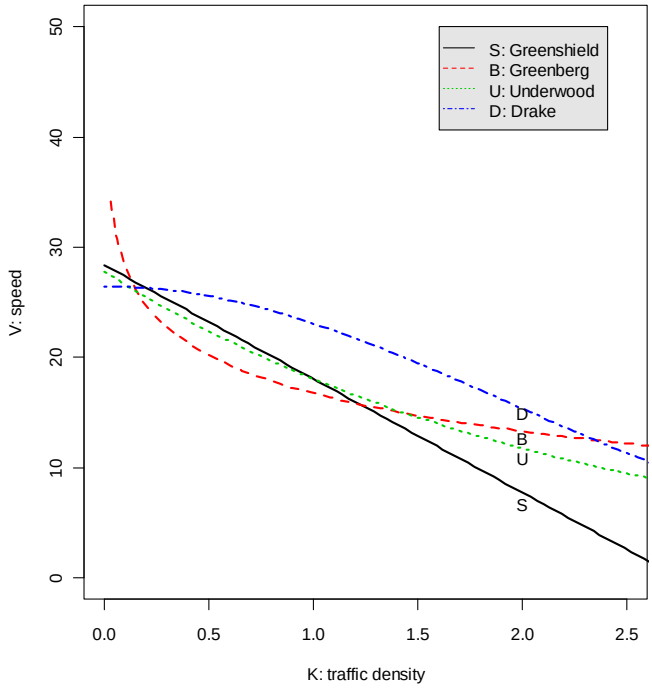

Figure 4. Speed-density relationship:
inner direction in loop routes at 0700-0800 hours

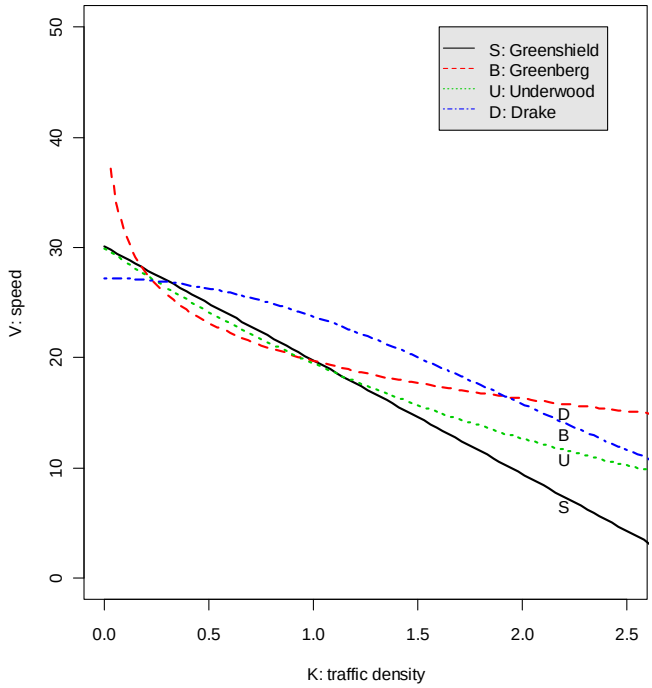

Figure 5. Speed-density relationship:
direction to center in radial routes at 0700-0800 hours

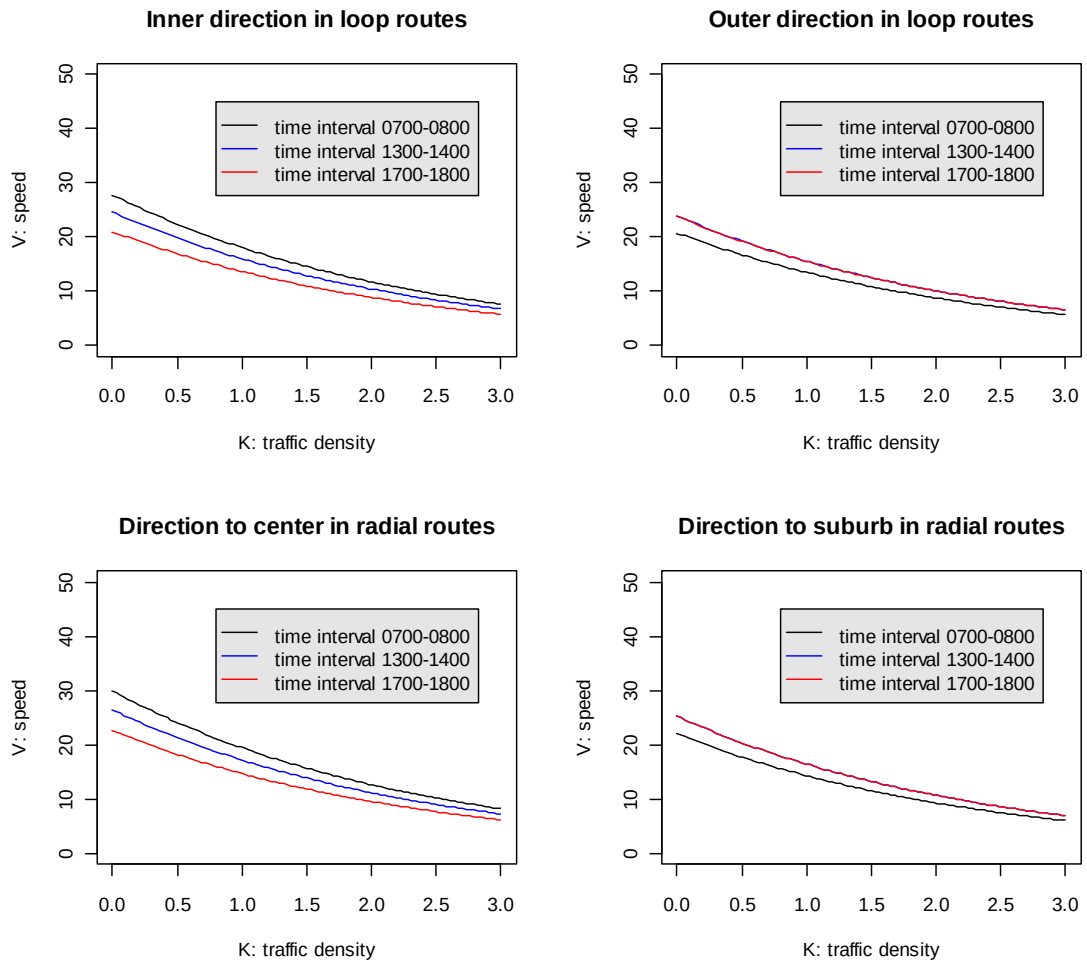

Figure 6. Speed-density relationship of Underwood Model